NEW FILAMENT DEPOSITION TECHNIQUE FOR HIGH STRENGTH, DUCTILE 3D PRINTED PARTS

Nicholas Rodriguez, Richard Crawford
Department of Mechanical Engineering, The University of Texas at Austin, Austin, TX 78712

Abstract

This paper proposes a method to use an off-the-shelf commercial Fused Deposition Modeling (FDM) 3D printer with minimal modifications to manufacture higher strength parts that fail in a ductile rather than brittle manner. A novel scan pattern designed to increase inter-layer adhesion in FDM parts is modeled and tested to determine its effect on mechanical properties of printed ABS parts. Results from three-point bend testing indicate a significant increase in part strength and elongation at break when using the proposed scan pattern compared to parts manufactured using a traditional scan pattern.

Background

Fused Deposition Modeling (FDM) is an additive manufacturing technique in which molten thermoplastic is selectively deposited in a layer-by-layer fashion to create freeform geometries. Within a single layer in the XY plane, a nozzle extrudes material along a pre-determined path given through G-Code commands. These G-Code commands are generated from a computer aided design (CAD) model of a part that has been sliced into layers using slicing software, and the commands contain information such as XYZ coordinates, extruder and bed temperatures, and filament feed and feed rate, or the amount and rate of deposition. The diagram of the extrusion process in Figure 1 shows how material is fed into a hot end, melted, and deposited onto the build plate and then pre-existing layers.

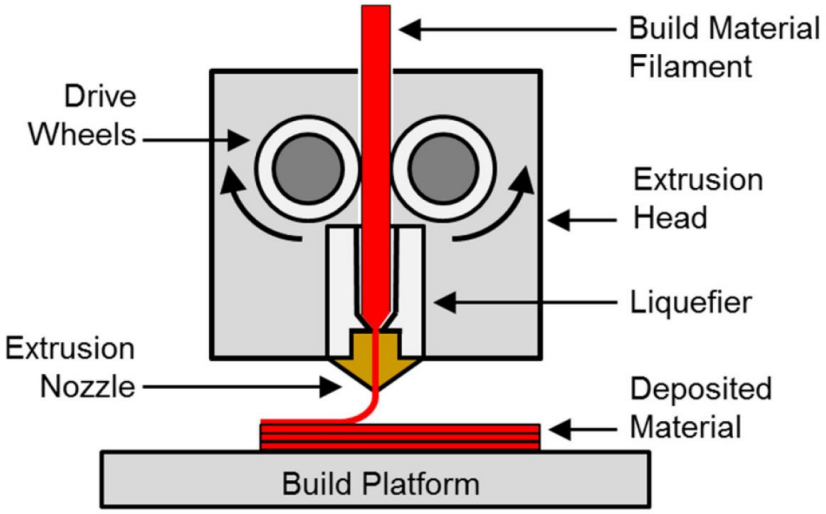

Figure 1: Filament Extrusion in FDM Process [1]

FDM has traditionally found extensive use with designers who desire to rapidly prototype a succession of iterative designs that are not intended to be functional. This is due to the limited number of materials that could be processed using FDM and the resulting reduced material

properties of a part compared to the material's bulk strength. Two main factors contribute to the reduction in material properties of printed parts: the existence of voids in the part in between deposition tracks or layers and the anisotropy seen in respective strengths of a deposited filament and its adhesion to neighboring tracks and between layers. Li studied the effect of voids on part strength and developed a relationship to relate the ratio of void space to part volume with end part strength. [2] Ahn and Bellini both varied numerous build parameters, including road width, air gap and part orientation, to determine their respective effects on part strength. Each found that parts built in the horizontal orientation (XYZ) had yield strengths two to four times greater than parts build vertically (ZXY), depending on air gap. [3] [4]

With the advent of recent process improvements and the use of new filaments with more desirable properties, FDM machines now find increasing use fabricating functional parts. Many techniques have been implemented to transform this technology from a prototyping technique to an end part fabrication technique. One such technique is printing with a fiber composite filament. Composite filaments can contain aramid, aluminum, glass, and carbon fibers and can have varying effects on material properties depending on fiber length, fiber orientation, and adhesion between fiber and matrix. Chopped carbon fiber additions in Nylon 12 have been shown to improve tensile stiffness and strength of thermoplastics by up to 100% in the axis of deposition. [5] [6] However, increases in material properties are typically not observed in the direction orthogonal to the build plane. For instance, in Stratasys' material data sheet, Carbon Fiber Nylon 12 has a tensile strength of 63.4 MPa in the XZ axis and 28.8 MPa in the ZX axis, compared to normal Nylon 12 with corresponding strengths of 32 and 28 MPa. While the in-plane strength is nearly doubled, the out of plane strength is hardly increased at all. This is to be expected as fiber composites only increase strength and stiffness along their orientation and should not be expected to increase layer adhesion. Various types of fiber composite printing exist, such as the Markforged (Cambridge, MA, USA) printers which use two nozzles to print fiber reinforced composites, one for the polymer matrix and one for the fiber. [7] Other printers use one nozzle to print a filament pre-impregnated with fibers such as the Dimension printers from Stratasys (Eden Prairie, MN, USA) whose part properties were discussed above. In addition to this distinction, various types of fibers are used for printing, including short chopped fibers (Stratasys) and continuous fibers. [8] Regardless of the method used to print fiber composites, parts tend to only experience increased strength and stiffness in the direction of filament deposition. [9]

Another method used to enhance FDM printing is printing with thermosets such as epoxies rather than thermoplastics. Compton studied deposition with an epoxy-based resin and carbon fiber filler. [10] Results indicated nearly isotropic materials with increased strength and stiffness over most thermoplastics. In addition, some injection molding processes use a two-part thermoset which chemically bonds to itself during mixing through crosslinking. In addition to printing enhanced materials, various post processing techniques involve altering the surface of the printed part after the printing process is completed. This can be accomplished through melting the surface and fusing layers together with an appropriate solvent or laminating the part with carbon fiber or another similar laminate. These techniques vary in labor and effectiveness, but can greatly increase strength, stiffness, and fatigue lifetime of a part. Finally, Belter showed increased strength and stiffness of 3D printed parts by printing parts containing voids and filling the voids with high strength resins. [11] These structures could be completely hollow or complex internal structures designed to reinforce particular areas. Although the chosen casting materials did not have much greater bulk properties, they are isotropic when molded and consequently can

reduce the anisotropy in printed parts. This process is time-consuming and geometry limited as material must be injected into the desired areas of the part and then sealed, but certain geometries had both greater strength and lower weight than solid printed ABS. While many of these techniques do succeed in augmenting the strength of FDM parts, most of them fall short in addressing layer delamination, the main failure mode of these parts. Most of the methods either increase in-plane strength or can be used to increase strength over a small portion of the part, but fail to address poor layer adhesion.

Additional relevant advances to the FDM printing process include machines and software enabling filament deposition on freeform surfaces. Curved layer slicing, proposed by Chakraborty, is a new slicing technique that eliminates the traditional flat layer deposition in previous FDM processes. [12] This new slicing technique allows tool paths to follow the curvature of the structure, rather than restricting their motion within a single horizontal plane. Demonstrated on a delta robot, parts manufactured using this method were seen to have a smoother surface finish than those manufactured using conventional slicing techniques. Choi developed a flexible FDM machine capable of depositing filament on freeform surfaces. [13] A portion of the study looked at bonding strength for a cylinder built on an already manufactured plate and found increased adhesion compared to that of the same cylinder adhered onto a plate using an adhesive recommended for FDM parts. Singamneni and Huang then studied material properties of parts fabricated using curved layer FDM and found increases in both strength and surface quality compared to flat layer FDM. [14] [15] This was tested using a modified three-point bend test specimen with a curved profile. One set of specimens was printed using traditional flat depositions while another followed the profile of the curved beam during printing. While this method does increase strength of the parts by providing a more uniform surface without stair stepping, it has not yet been used to address the inherent anisotropy of FDM parts.

In addition to having different strength and stiffness in plane compared to transversely, the anisotropic nature of 3D printed materials also has a detrimental effect on the failure mechanism of printed parts. When parts fail through layer delamination, the failure occurs suddenly and catastrophically, without any plastic deformation. This brittle behavior of otherwise ductile parts makes it difficult to predict the moment or degree of failure or to design for fatigue failure modes in order to anticipate and prevent this predisposition to sudden structural failure. Gorski demonstrated how part orientation has not just a significant influence on final strength of the part, but also on macroscopic material behavior. [16] He determined a series of transition points, based on part orientation, in which parts under various loading conditions, including tensile and flexural loads, experience failure mechanism transitions from ductile yielding to brittle fracture. This transition was accompanied by a reduction of 50% in both yield strength and elongation at break when changing from horizontal to vertical build orientations. As the results of his study indicate, it is evident that a method must be developed to reduce the anisotropy of FDM printed parts, regardless of the material used.

Modeling Orthotropy of Additively Manufactured Parts

All additive manufacturing processes that are layer-based manufacturing methods exhibit orthotropic tendencies in their properties. In particular, an FDM part can be viewed as a laminated composite consisting of ABS layers with multi-directional properties. The part will exhibit one set of properties along the direction of the deposition, another set orthogonal to the deposition path but in the same layer, and a third set spanning across layers. The in-plane differences in material

properties is mitigated in practice through incorporating a 0-90 offset in the scan pattern, in which each layer alternates the orientation of filament deposition 90 degrees offset to the previous layer. This allows each layer to be considered as having continuous material properties such that the anisotropy is only found between the in-plane and orthogonal directions. Therefore, FDM printed parts can be considered to be transversely isotropic; the physical properties within one plane (the XY plane) are isotropic and symmetric about the axis orthogonal to the plane (Z axis).

Using Hooke's law and assuming linear elasticity, stress and strain can be related through a 36 component compliance matrix. By reflecting and rotating the matrix about its planes of symmetry and equating equivalent states, the number of independent coefficients in the compliance matrix can be reduced depending on its geometry. For a transversely isotropic material, the compliance matrix reduces to five independent coefficients: E_x, E_z, G_{yz}, v_{zx} (= v_{xz}), v_{yx} (= v_{xy}), shown in Figure 2.

$$\underline{\underline{C}} = \begin{bmatrix} C_{11} & C_{12} & C_{13} & 0 & 0 & 0 \\ C_{12} & C_{11} & C_{13} & 0 & 0 & 0 \\ C_{13} & C_{13} & C_{33} & 0 & 0 & 0 \\ 0 & 0 & 0 & C_{44} & 0 & 0 \\ 0 & 0 & 0 & 0 & C_{44} & 0 \\ 0 & 0 & 0 & 0 & 0 & (C_{11}-C_{12})/2 \end{bmatrix} \quad \underline{\underline{C}}^{-1} = \begin{bmatrix} \frac{1}{E_x} & -\frac{\nu_{yx}}{E_x} & -\frac{\nu_{zx}}{E_z} & 0 & 0 & 0 \\ -\frac{\nu_{xy}}{E_x} & \frac{1}{E_x} & -\frac{\nu_{zx}}{E_z} & 0 & 0 & 0 \\ -\frac{\nu_{xz}}{E_x} & -\frac{\nu_{xz}}{E_x} & \frac{1}{E_z} & 0 & 0 & 0 \\ 0 & 0 & 0 & \frac{1}{G_{yz}} & 0 & 0 \\ 0 & 0 & 0 & 0 & \frac{1}{G_{yz}} & 0 \\ 0 & 0 & 0 & 0 & 0 & \frac{2(1+\nu_{xy})}{E_x} \end{bmatrix}$$

Figure 2: Compliance matrix for transversely isotropic materials [17]

These values were determined both experimentally and from published data that matches the material properties of printed parts. Flexural bars to determine Young's modulus longitudinally and transversely were manufactured using a Delta style FDM printer, the Rostock Max (SeeMeCNC, Ligonier, IN, USA). Test specimens were manufactured according to ASTM D790 and printed in acrylonitrile butadiene styrene (ABS), a common thermoplastic used in 3D printing. FDM printers intake a G-Code file which contains simple commands such as XYZ positions, extruder movement, and movement speeds. These G-Code files can be created through slicing software, such as Slic3r (an open-source slicing program), from an STL file containing 3D geometric data for any given part. Eight flexural bars were printed in both the horizontal (XYZ) and vertical (ZXY) orientations at a layer height of 0.2mm. In order to print the specimens vertically at such a high aspect ratio without any lateral swaying during printing, the beams had small bridges linking them together, increasing the print's effective footprint. Flexural testing was conducted on both sets of specimens at a strain rate of 13.5 mm/mm/min, calculated from ASTM D790 based on the part geometry. [18] Further discussion of the experimental method is given in the following section. Table 1 shows the results from initial flexural testing.

Table 1: Experimental material properties for 3D printed ABS

Orientation	Young's Modulus (MPa)	Ultimate Flexure Strength (MPa)	Percent Elongation at Break
ZXY	1578±139	43.1±6.4	3.33±0.49
XYZ	2358±80	74.9±1.7	9.99±0.71

After the average flexural modulus of the printed part was determined, Poisson's ratios and the shear modulus values were determined by matching experimental data acquired from flexural testing to a series of published data to find the best match. Rodriguez conducted extensive testing on 3D printed ABS with similar results, so his were used to complete the model. [19] The full set of material properties used in the model is given in Table 2.

Table 2: Material properties for 3D printed ABS used in model

	X	Y	Z
Young's Modulus (MPa)	2358	2358	1578
	XY	YZ	XZ
Poisson's Ratio	0.268	0.339	0.339
Shear Modulus (MPa)	930	678	678

Modeling and Experimentation of Layer Spanning Deposition for Flexural Test Specimens

The proposed layer spanning deposition is meant to decrease the anisotropy inherent in additively manufactured parts by increasing the strength across layers in the transverse direction. The deposition technique is similar to the already used 0-90 offset between subsequent layers' raster pattern seen in Figure 3 below, but expanded to the third principal direction. By depositing material in the Z direction, spanning across previously printed layers, parts will exhibit closer to isotropic material properties. The layer spanning deposition technique is shown below on the right contrasted with a traditional 0-90 alternating scan pattern on the left.

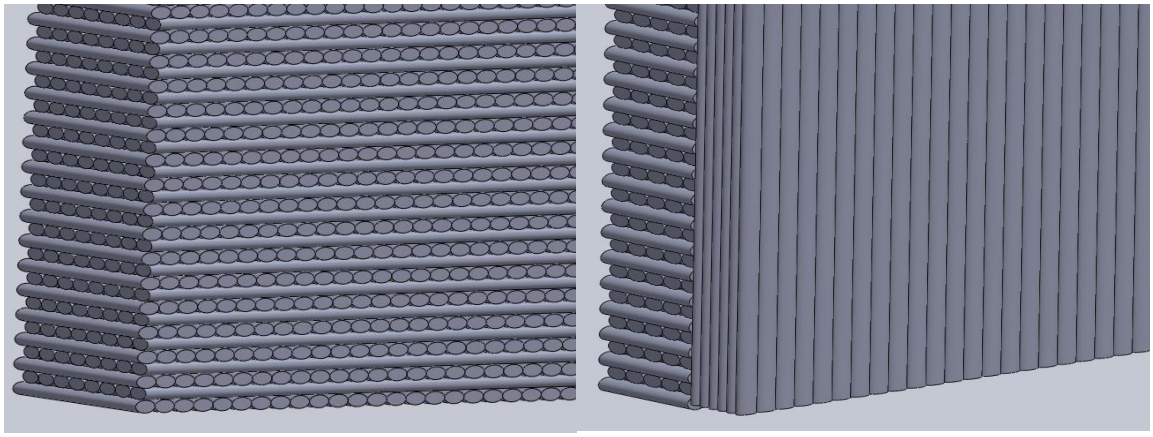

Figure 3: Traditional deposition pattern (16-0) and layer spanning deposition pattern (10-6)

This study consists of finite element analysis using experimental data from 3D printed flexural bars in order to predict macroscopic behavior of parts printed using layer spanning

deposition. Three sets of models, in addition to the vertical and horizontal flexural bars, were analyzed using ANSYS (Canonsburg, PA, USA): 87.5% ZXY, 75% ZXY, and 62.5% ZXY, with the remaining portions of each model built in XYZ. These models are hereafter referred to as 16-0, 14-2, 12-4, 10-6, and 0-16 denoting the ratio of layer thickness deposited in the ZXY orientation compared to XYZ.

Modeling

Geometries were created in SolidWorks (Dassault Systèmes Solidworks Corp., Waltham, MA, USA) and consist of a single beam dimensioned according to ASTM D790 (125mm x 12.7mm x 3.2mm) and three cylinders representing the three contact points in the flexural test. The geometries were imported into ANSYS and appropriate coordinate systems were applied to the two bodies that made up the beam, with the Z axis oriented along the vertical print direction of each respective component. This ensured each body was modeled using the appropriate anisotropic material properties. Contact between the two support cylinders and the beam was modeled as frictionless contact, allowing the beam to slide tangentially to its contact points but preventing loss of contact between the beam and cylinders. The top cylinder and beam were modeled with friction contact to ensure a soft constraint that limits the beam's sliding during initial application of the load. The two bodies that make up the beam were modeled with bonded constraints to prevent any relative movement between the surfaces; this is appropriate for modeling elastic behavior as the internal structure of the beam is not plastically deforming, so there should be no slip between the surfaces. The two bottom cylinders were modeled as fixed supports while the top cylinder was given an applied deformation in the negative Z axis, with movement in the other directions fixed. Initially, two vertices in the middle of the beam were fixed in the X and Y direction but allowed to freely move in the Z direction. This was intended to ensure the beam only deflected downwards since movement was constrained in the other two axes, but it was found to create a stress singularity at the vertices as those nodes were not allowed to translate as the elements deformed during analysis. The intended outcome of constraining movement in the X and Y directions was achieved instead through the friction contact stated above, in addition to prohibiting the beam's rotation about the Z axis. A convergence study was conducted to verify appropriate mesh size for each model, and it was determined that between each surface there should be at least two elements to properly analyze the model. For the 10-6 sample, two meshes were studied consisting of 4,174 and 30,403 elements and are shown in Figure 4.

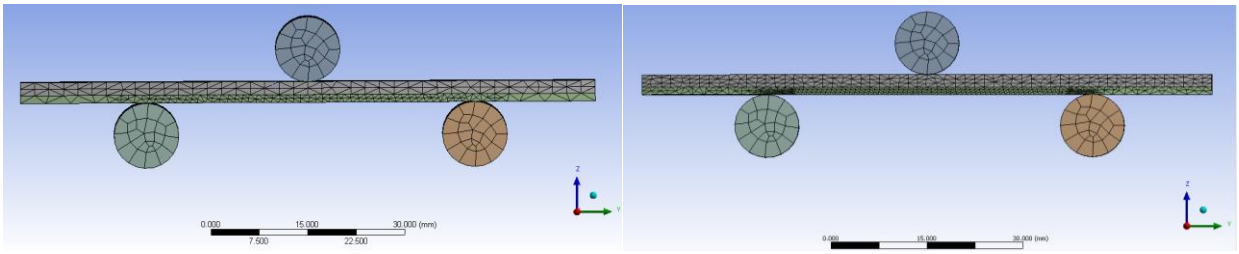

Figure 4: Two meshes of 10-6 specimen

The resulting maximum stresses at a 5mm displacement were 82.095 and 82.063 MPa, showing only a negligible difference. These conditions and mesh settings were used to model all five cases and stress, strain, and force at the supports were monitored throughout the analysis to compare to later experimental results.

Experimentation

Following analytical modeling, flexural specimens were manufactured using a combination of traditional FDM deposition and the proposed layer spanning deposition to match each finite element model. The 16-0 vertically oriented specimens were sliced using a typical 0/90 offset raster pattern between layers, as is common in many slicing programs, to eliminate in-plane anisotropy. The other sets of beams required a portion of the specimen to be manufactured similarly to the first set, but with a second layer of material deposited afterwards. This second layer consisted of longitudinal depositions all running the same direction, across the previously deposited layers. To accomplish this, the parts were laid on their sides and adhered to the build plate, while the printer was set to have a Z-offset equal to the thickness of the already printed model. The G-Code for this second portion of printing was modified, as typical slicing software does not give the option to deposit subsequent layers without having the raster pattern shift 90 degrees each layer. Without modification, the initial G-Code would have resulted in alternating depositions that first spanned the layers and then were parallel to the layers as seen in Figure 5.

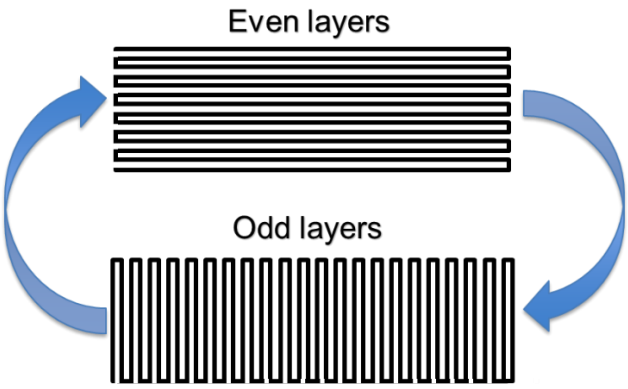

Figure 5: Zero and 90 degree offset in subsequent layers

By replacing every other layer's G-Code with the previous layer's code while only altering the print height, the printer deposited a series of layers of filament all spanning across the ZXY layers. The results of this modification can be seen in the comparison between an unmodified and a modified G-Code rendering in Figure 6.

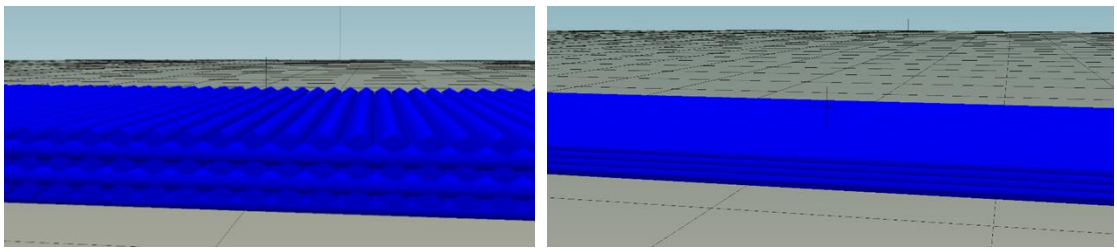

Figure 6: Unmodified and modified G-Code for layer spanning deposition

After printing all five sets of specimens, they were each were tested on the Instron (Norwood, MA) mechanical testing machine using a 3-point bend test fixture with a span length

of 50mm. From ASTM D790 and the part geometry, a strain rate of 13.5 mm/mm/min was determined to be appropriate and the parts were tested to failure. Displacement was measured through crosshead movement, which is an accurate measurement for specimens with a relatively low stiffness compared to the Instron's load frame.

Results

For each specimen from the 3-point bend tests, stress and strain were calculated according to equations 1 and 2. The resulting plots of stress vs strain are shown below in Figure 7 and reveal the different methods in which varying amounts of layer spanning deposition change the material properties of a printed part.

$$\sigma = \frac{3FL}{2bd^2} \tag{1}$$

$$\varepsilon = \frac{6Dd}{L^2} \tag{2}$$

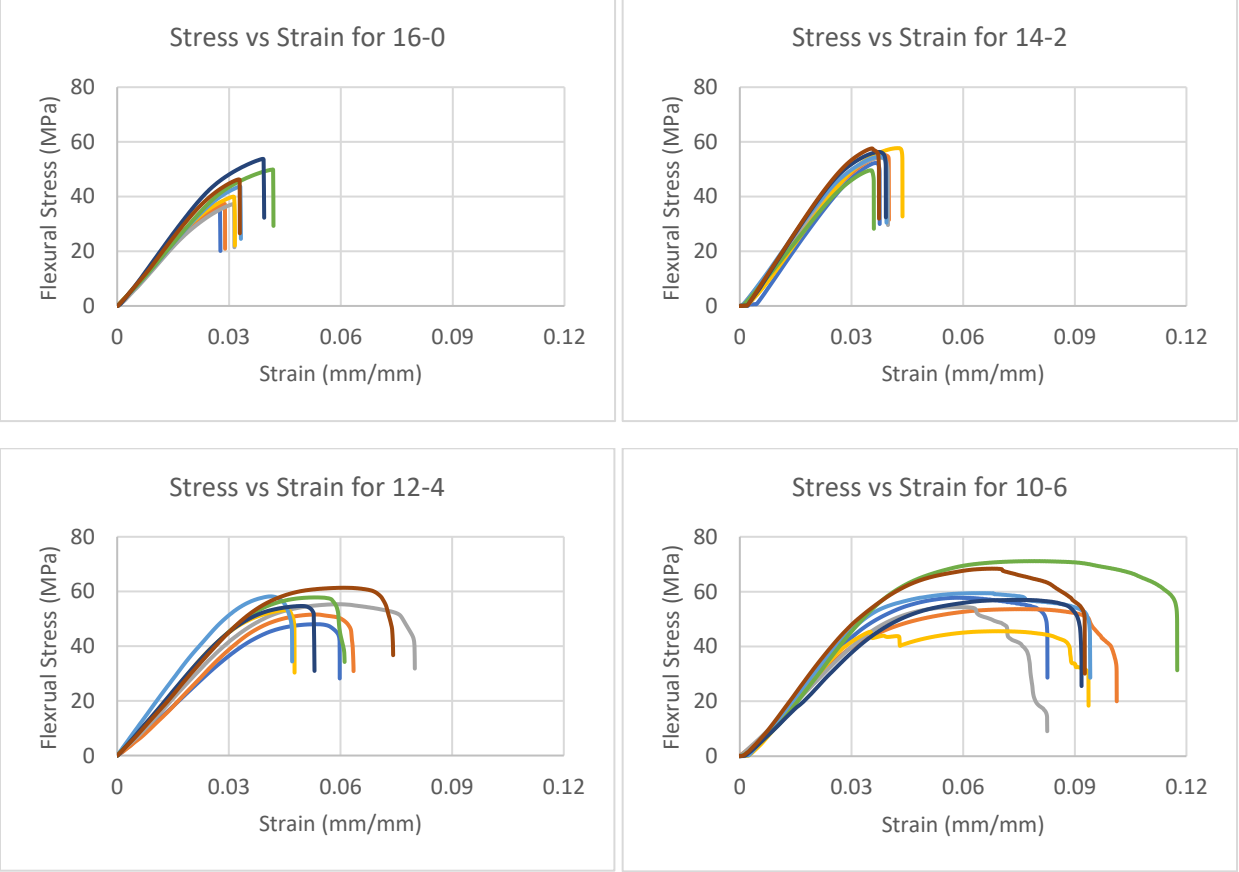

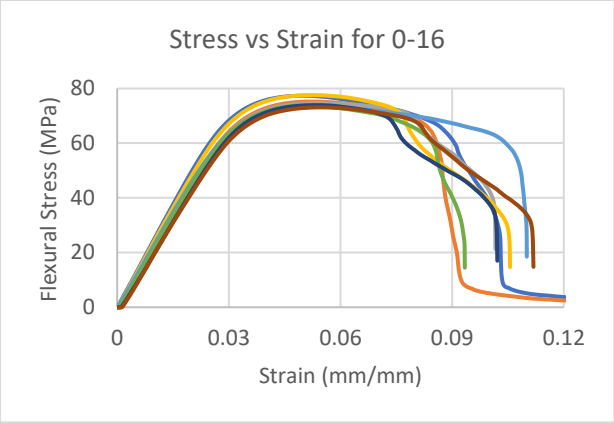

Figure 7: Stress vs strain plots for 5 sets of flexural specimens

In addition, for each set of data, the average yield stress was calculated based on a line offset 0.2% and parallel to the slope. The average calculated yield strengths for each set are shown in Figure 8.

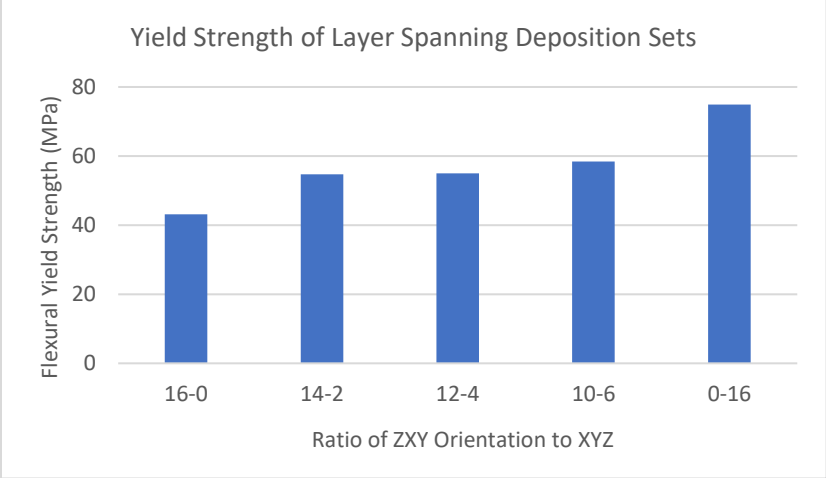

Figure 8: Yield Strength of layer spanning deposition parts

The calculated strain was used to determine elongation before breaking for the varying ratios of normal deposition to layer spanning deposition. Strain at break was chosen as the strain at which a specimen still held 40% of its maximum load. Values for each set of specimens are shown in Figure 9.

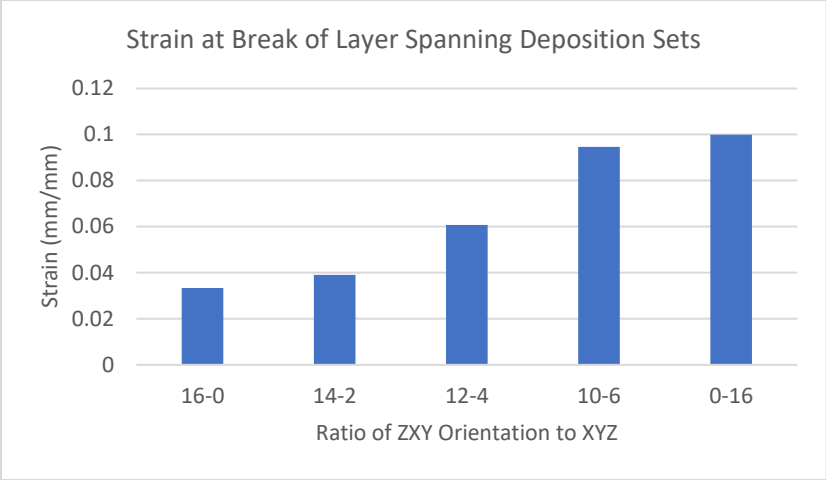

Figure 9: Strain at break of layer spanning deposition parts

As seen in the above two figures, flexural specimens with a higher portion of their thickness manufactured in the XYZ orientation that spans the vertical layers exhibited both higher yield strength and a larger elongation at break. This also reveals that the specimens with layer spanning deposition experience a different failure mode than the traditional parts. Such parts are ductile and yield plastically before fracturing rather than just deforming elastically and fracturing in a brittle manner. This is to be expected due to the relatively ductile behavior of a continuously deposited filament compared to the brittle failure mechanism of layer delamination seen in the samples with the least layer spanning deposition. This concept is demonstrated even more clearly in further samples that were printed on an older FDM printer, the Solidoodle 3 (Brooklyn, NY, USA). As shown in Table 3, yield strength and strain at break increase with layer spanning deposition to an even greater degree than seen in parts printed on the Rostock Max.

Table 3: Material properties for flexural specimens printed on Solidoodle 3

Fractional Width ZXY	Fractional Width XYZ	Yield Strength (MPa)	Strain at Break
16	0	8.84	.020
12	4	35.4	.065

This could be because parts produced by this printer tended to have an increased surface roughness compared to those produced by the newer Rostock Max. This surface roughness is likely due to the difference between a lead screw actuated Z-stage in the Cartesian style Solidoodle compared to the carriage and linkage driven hot-end of the Delta style Rostock. Any deviation of the lead screw from complete straightness results in lateral translation of the vat correlated to its height and increases the surface roughness. This causes imperfections as seen in Figure 10 which enhance the inherent orthotropic nature of FDM parts, as inter-layer failures are expected to occur more frequently with greater imperfections. From these results, layer spanning

deposition should be expected to mitigate failure due to imperfections in printing while reducing anisotropy in printed parts.

Figure 10: Flexural specimen built on Solidoodle 3 (left) and Rostock Max V3 (right)

Furthermore, results from finite element analysis of each test specimen are compared to experimental data to validate accuracy of the model. Maximum stress and strain are both expected to occur at the center bottom edge during testing and were monitored during analysis. An example plot of maximum stress demonstrating this for the 0-16 specimen is shown in Figure 11.

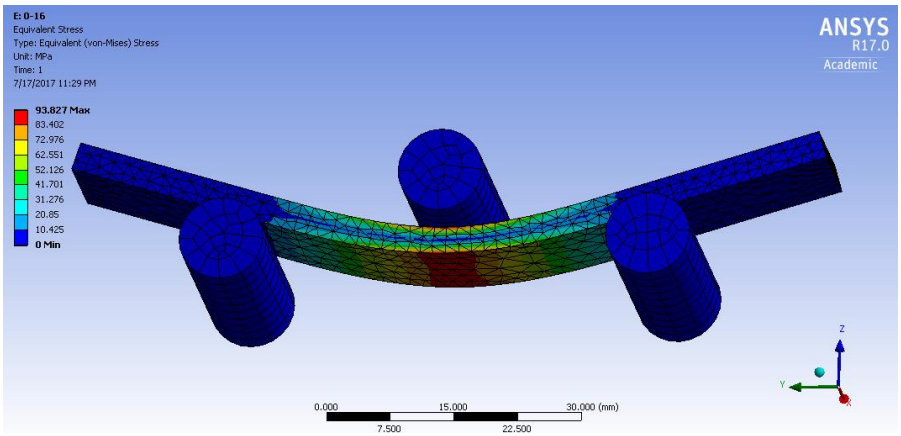

Figure 11: Maximum stress for 0-16 specimen under 5 mm displacement

Stress was then plotted against elongation in the expected elastic region and compared to the model, as seen in Figure 12.

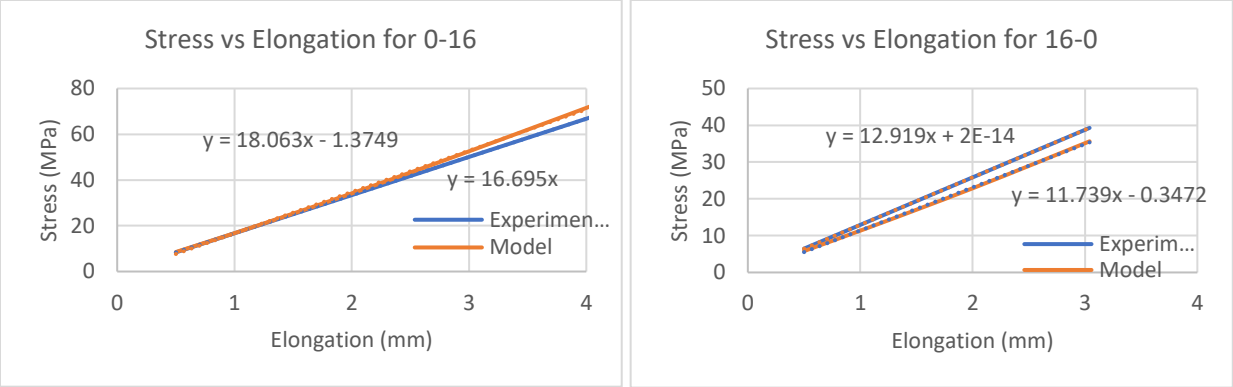

Figure 12: Model and experimental data for stress vs elongation

From the slopes of these two plots, the errors between the model and experimental data are 7.5% and 9.1% respectively.

Conclusions and Future Work

FDM printing using a combination of layer spanning deposition and traditional deposition has been shown to increase material properties in 3D printed parts. After modeling 3-point bend test parts and conducting tests on a series of specimens while varying the ratio of traditional to layer spanning deposition, results indicate that an increasing percentage of thickness built using layer spanning deposition results in increased yield strength and a shift from brittle fracture to ductile yielding, with an increasing elongation at break. Since a finite element model of 3D printed parts has been verified through experimental data, one can design parts to incorporate layer spanning deposition in order to maintain the same geometry and mass, but vary structural behavior depending on desired use. This enables design optimization through not only material placement, but also material orientation.

Future work consists of first verifying that similar structural enhancements result from layer spanning deposition on more complex geometries than a flat beam. Using curved layer slicing, material can be deposited on non-planar surfaces, following the curvature of a wider range of geometries. In addition, this technique will be demonstrated on not just the top surface of a printed part, but around the entire outer surface. This will require a hardware modification to an off-the-shelf printer to enable depositing filament around an entire part.

Reference List

1. Cantrell J. et al. (2017) Experimental Characterization of the Mechanical Properties of 3D Printed ABS and Polycarbonate Parts. In: Yoshida S., Lamberti L., Sciammarella C. (eds) Advancement of Optical Methods in Experimental Mechanics, Volume 3. Conference Proceedings of the Society for Experimental Mechanics Series. Springer, Cham.

2. Li, L., Sun, Q., Bellehumeur, C., and Gu, P. (2002), "Composite Modeling and Analysis for Fabrication of FDM Prototypes with Locally Controlled Properties." *Journal of Manufacturing Processes*. Vol. 4, Num. 2. p.p. 129-141.

3. Ahn, S.-H. et al (2002), "Anisotropic material properties of fused deposition modeling ABS." *Rapid Prototyping Journal*. Vol. 8, Num. 4, p.p. 248–257.

4. Bellini, A. and Güçeri, S. (2003), “Mechanical characterization of parts fabricated using fused deposition modeling.” *Rapid Prototyping Journal*. Vol. 9, Num. 4, p.p. 252–264.

5. FDM Nylon 12. *Stratasys.* (2014) http://www.stratasys.com/materials/fdm/nylon.

6. FDM Nylon 12CF DATA SHEET. *Stratasys*. (2017) http://www.stratasys.com/nylon12cf.

7. The Mark Two. *Markforged*. (2017) https://markforged.com/mark-two/.

8. Matsuzaki, R. et al. (2017), “Three-dimensional printing of continuous-fiber composites by innozzle impregnation.” Scientific Reports Vol. 6, Num. 23058, p.p. 1-7.

9. Tekinalp, H.L., et al. (2014), “Highly oriented carbon fiber–polymer composites via additive manufacturing.” *Composite Science and Technology*. Vol. 105, p.p. 144-150.

10. Compton, B.G., and Lewis, J.A. (2014), “3D-Printing of Lightweight Cellular Composites.” *Advanced Materials*. Vol. 2, Num. 34, p.p. 5930-5935.

11. Belter, J.T., and Dollar, A.M. (Sept. 2014), “Strengthening of 3D Printed Robotic Parts via Fill Composting.” Proceedings of the International Conference on Intelligent Robots and Systems (IROS). Chicago, IL.

12. Chakraborty, D. (2008), “Extruder path generation for Curved Layer Fused Deposition Modeling.” *Computer Aided-Design*. Vol. 40, Num. 2, p.p. 235-243.

13. Choi, J.W., Medina, F., Kim, C., Espalin, D., Rodriguez, D., Stucker, B., and Wicker, R. (2011), “Development of a mobile fused deposition modeling system with enhanced manufacturing flexibility.” *Journal of Materials Processing Technology.* Vol. 211, Num. 3, p.p. 424-432.

14. Singamneni, S., Roychoudhury, A., Diegel, O., and Huang, B. (2012), “Modeling and evaluation of curved layer fused deposition.” *Journal of Materials Processing Technology*. Vol. 212, Num. 1, p.p. 27-35.

15. Huang, B. (2009), “Development of a software procedure for Curved Layered Fused Deposition Modelling (CLFDM)” *ETD Collection for AUT University, Auckland, New Zealand*.

16. Gorski, F. (2015), “Strength of ABS Parts Produced by Fused Deposition Modelling Technology–A Critical Orientation Problem.” *Adv. Sci. Technol. Res. J.* 2015; 9(26):12 –19.

17. Lekhnitskii, S. G. (1963), “Theory of Elasticity of an Anisotropic Elastic Body.” Holden-Day Inc., San Francisco.

18. ASTM (2015), ASTM D790-15, Standard Test Methods for Flexural Properties of Unreinforced and Reinforced Plastics and Electrical Insulating Materials, ASTM.

19. Rodriguez, J.F., Thomas J.P., and Renaud J.E. (2003), “Mechanical behavior of acrylonitrile butadiene styrene (ABS) fused deposition materials modeling.” *Rapid Prototyping Journal.* Vol. 7, Num. 3, p.p. 148-158.